Planar Rotor-Enabled Quenching-Resistant NIR-II Fluorophores for High-Contrast Bioimaging and Efficient Cancer Phototheranostics

Weilong Chen[a], Sa Wang[b], Hanumantha Rao Ganipisetti[c], Ka-Wai Lee[a], Zhiqiang Guan[a], Siyu Chen[b], Yuqing Li[a], Chuang Zhang[b], Yeteng Zhong[e], Jinfeng Zhang[b], Ken-Tsung Wong*[cd], Yingpeng Wan*[a], Chun-Sing Lee[a]*

[a]Center of Super-Diamond and Advanced Films (COSDAF)

Department of Chemistry, City University of Hong Kong

83 Tat Chee Avenue, Kowloon, Hong Kong SAR 999077, P. R. China

E-mail: ypwan3@cityu.edu.hk

[b]Key Laboratory of Molecular Medicine and Biotherapy

School of Life Science, Beijing Institute of Technology

Beijing 100081, P. R. China

E-mail: jfzhang@bit.edu.cn

[c]Department of Chemistry, National Taiwan University, Taipei 10617, Taiwan

E-mail: kenwong@ntu.edu.tw

[d]Institute of Atomic and Molecular Science Academia Sinica, Taipei 10617, Taiwan

[e]CAS Key Laboratory for Biomedical Effects of Nanomaterials and Nanosafety, CAS Center for Excellence in Nanoscience, National Center for Nanoscience and Technology, Chinese Academy of Sciences, Beijing 100190, P. R. China

Table of Content

1. Methods and materials

All chemicals are purchased from Energy Chemical or Aldrich and used as received unless otherwise mentioned. ^{1}H NMR and ^{13}C NMR spectra are recorded on 400/600 MHz Bruker spectrometers. The mass spectrum is measured by Bruker Daltonics autoflex speed Mass Spectrometer. Absorption spectra of molecules and nanoparticles (NPs) are measured by an absorbance spectrometer (Shimadzu 1700). Fluorescence spectra of molecules and NPs are measured by a spectrofluorometer (Edinburgh FLS980). Size distribution and zeta potential of NPs are tested by a dynamic light scattering particle size analyzer (Malvem Zetasizer Nano ZS). Morphologies of the obtained NPs are characterized by a transmission electron microscope (Philips Technai 12). Powder X-ray diffractometer (Bruker D2 PHASER) was carried out using a LYNXEYE XE-T detector at room temperature scanned from 10° to 75° at a speed of 1° min^{-1}. Temperature-dependent photoluminescence lifetime measurements were carried out using an Edinburgh Instruments FLS980 spectrometer equipped with a variable-temperature cryostat. The sample was mounted in a sealed quartz cuvette and placed inside the cryostat chamber, which allowed precise control of the temperature from 77 K to 350 K. Excitation was provided by a 670 nm EPL laser and detection wavelength of lifetime is 780 nm. Photothermal images and the temperature of the solution samples are recorded by a thermal imaging camera (Fluke Ti400). Confocal images are collected using a laser confocal scanning microscope (Leica SPE).

2. Theoretical calculation

All theoretical calculations are performed on the Gaussian 16_A03 package.[1] For density-functional theory calculations, ground-state (S_0) molecular geometries are optimized at M06-2X/6-311G(d) level. The HOMO and LUMO are then calculated based on the optimized S_0 molecular geometries at the same level to further investigate the rotors of molecules, relative energies of the specific dihedral angle rotation are scanned from the s-*cis* conformation to the s-*trans* conformation.

3. Preparation of NPs

The stock solution of Y6 molecules (1 mg/mL) is prepared by dissolving molecules into THF. Pluronic F127 in THF (4 mL, 5 mg/mL) is then mixed with Y6 stock solution (2 mL) by sonication. The mixture is rapidly dropped into deionized water (54 mL) under stirring. The mixture is stirred overnight to remove the THF solvent completely. Then, Y6 NPs dispersion is ultra-filtered with centrifugal filter units (Millipore, size of 100 kDa) to obtain a concentrated NPs solution. Finally, the concentrated Y6 NPs dispersion is stored at 4 °C in the dark for long-term usage. BTP-2TCF NPs are prepared in the same way.

Concentration of NPs is measured by the standard curve of molecules. Standard curves of molecules in THF with varied concentrations are first obtained. Then, the optical densities of the absorption peak are plotted against solution concentration to get

equation 1. After that, NPs dispersion is dissolved back in THF and the corresponding optical density of the absorption peak is substituted into equation 1 to calculate the NPs concentration:

$$y = C + \varepsilon x \quad (1)$$

where y is optical density, x is concentration, C and ε are constant and extinction coefficient, respectively.

4. Calculation of NIR-II photoluminescence quantum yield

The photoluminescence quantum yield (PLQY) of Y6 NPs and BTP-2TCF NPs are determined using IR26 as a reference, with a PLQY value of 0.5 % in 1,2-dichloroethane (DCE).[2] IR26 is dissolved in DCE to prepare five samples with different optical density (OD) at 808 nm (~0.02, ~0.04, ~0.06, ~0.08, and ~0.1). Subsequently, the NIR-II fluorescence spectra are collected by the Edinburgh FLS980 and both the obtained spectra are integrated within the wavelength range of 900-1500 nm. The emission spectra of Y6 NPs and BTP-2TCF NPs dispersions are obtained and integrated by the same method. Finally, the integrated fluorescence intensity is plotted against OD at 808 nm. The PLQY is calculated by using the following equation (2):

$$QY_{sample} = QY_{ref} \cdot \frac{slope_{sample}}{slope_{ref}} \cdot \left(\frac{n_{sample}}{n_{ref}}\right)^2 \quad (2)$$

where QY_{sample} is the PLQY of Y6 NPs / BTP-2TCF NPs with a wavelength of 900-1500 nm, QY_{ref} is the PLQY of IR26, $slope_{sample}$ is the slope obtained by linear fitting of the integrated fluorescence intensity of Y6 NPs/ BTP-2TCF NPs within the 900-1500 nm wavelength range against the OD at 808 nm, $slope_{ref}$ is the slope obtained by linear fitting of the integrated fluorescence intensity of IR26 with a wavelength of 900-1500 nm against the OD at 808 nm, n_{sample} is the refractive indices of water, and n_{ref} is the refractive indices of DCE. For comparison of PLQY between molecules and NPs, 690 nm xenon light is used.

Absolute PLQY was determined using an integrating sphere setup, which enables collection of all emitted and scattered photons regardless of direction. Measurements were performed under identical excitation conditions for blank, reference, and sample, allowing quantification of absorbed excitation photons and emitted fluorescence photons. The PLQY was then calculated as the ratio of total emitted photons to absorbed photons, ensuring accurate and reproducible values.

5. Assessment of reactive oxygen species generation

Method of comparing singlet oxygen generation of two molecules in THF (Figure S14, Figure 4D): 1,3-Diphenylisobenzofuran (DPBF) probe is used to characterize the singlet oxygen generation. A 3 mL THF solution containing the target molecules and the DPBF probe was irradiated at 750 nm with a power density of 160 mW/cm^2 for a total duration of 50 seconds, applied in 10-second intervals. For consistency, the initial absorbance of the DPBF probe in the testing solution was adjusted to 1.0 at 415 nm, while the optical density of the molecules within the system was standardized to 0.058 at 750 nm. Samples are irradiated with a 750 nm laser, as Y6

and BTP-2TCF molecules show negligible absorption at 808 nm.

Method of comparing superoxide radicals generation of two molecules in THF (Figure S15A, B&C): Dihydrorhodamine 123 (DHR 123) probe is utilized to detect the superoxide radicals. In 3 mL THF solution, 30 μL DHR 123 (stock concentration: 1mM) is added. The concentration of the molecules was adjusted such that the final optical density of the solution at 750 nm was 0.161. Both the control and experimental groups were subsequently irradiated with a 750 nm laser at a power density of 160 mW/cm^2, applied in 10-second intervals. The fluorescence intensity of DHR 123 is recorded under 460 nm excitation.

Method of comparing hydroxyl radicals generation of two molecules in THF (Figure S15D, E&F): Hydroxyphenyl fluorescein (HPF) probe (stock concentration: 2.36 mM) is used to verify the generation of hydroxyl radicals. 12.5 μL HPF is introduced into 3mL molecule solution to carry on the experiments. The final optical density of the solution at 750 nm was adjusted to 0.166. Both the control and experimental groups were subsequently irradiated with a 750 nm laser at a power density of 160 mW/cm^2, applied in 10-second intervals. The fluorescence intensity of DHR 123 is recorded under 460 nm excitation.

Method of measuring singlet oxygen generation of NPs in water (Figure S25, Figure 4E): To estimate the distinct ability of singlet oxygen generation between the molecules in THF and NP in water, DPBF probe is also used in the NPs systems. To ensure that the molar concentration of molecules in the NP system matched that in the dilute THF solution (Figure S14, Figure 4D), 3.2 μL of 0.77 mM Y6 NPs (the same concentration as Y6 in THF when optical density is 0.058 at 750 nm) and 13.3 μL of 0.61 mM BTP-2TCF NPs (the same concentration as BTP-2TCF in THF when optical density is 0.058 at 750 nm) were individually introduced into the aqueous solution containing the DPBF probe (initial absorbance of the DPBF probe in the testing solution was first adjusted to 1.0 at 415 nm). The NPs solutions containing molecules and probe are excited by 750 nm laser (160 mW/cm^2, the same condition as Figure S14 and Figure 4D) for 50 s with a time interval of 10 seconds.

Method of evaluating total ROS generation of NPs in water (Figure S16, Figure 3E&3F): To test the total reactive oxygen species (ROS) generation of NPs, 2',7'-dichlorodihydrofluorescein diacetate (DCFH-DA, 1.2 mg) is first dissolved in ethanol (2.5 mL) and mixed with NaOH (0.01 M, 10 mL). After 30 minutes, the mixture is diluted with phosphate-buffered saline (PBS, 50 mL) to prepare the DCFH stock solution stored at -20 °C in the dark for long-term use. NPs dispersion is added into DCFH stock solution to yield a final optical density of 0.32 at 808 nm. Subsequently, the NP solution was irradiated with an 808 nm laser at a power density of 500 mW/cm^2, applied in 30-second intervals. The emission spectra of oxidized 2',7'-dichlorofluorescein (DCF) are collected by the Horiba-Duetta (λ_{ex} = 460 nm, λ_{em} = 480-700 nm).

Method of evaluating singlet oxygen quantum yield of NPs in water (Figure S26): Singlet oxygen quantum yield (ΦΔ) of Y6 NPs and BTP-2TCF NPs are measured using commercial ICG as a reference (0.2%). 3 mL water containing ICG/Y6 NPs/BTP-2TCF NPs and DPBF probe are excited by 808 nm (200 mW/cm^2) for 50 seconds with

an interval of 10 seconds. The initial absorption of the DPBF probe in the testing solution is set as ~1.0 at 415 nm, while the final optical density of molecules in the testing system is set as 0.20 at 808 nm. The experiments are conducted in the dark.

6. Excited-state dynamic behaviour

Excited-state dynamic behaviors of Y6 and BTP-2TCF NPs were characterized by femtosecond transient absorption. The NPs samples (35 μmol/L) are excited by a 700 nm pump laser irradiation. Normalized kinetic curve of Y6 NPs and BTP-2TCF NPs at representative wavelength within GSB region. The decays are fitted by the following function:

$$I = A1e^{-t/\tau_1} + A2e^{-t/\tau_2}. \quad (3)$$

7. Photothermal properties

Y6 NPs dispersion is diluted to various concentrations in a total volume of 1 mL. Subsequently, the temperature of each sample is recorded during excitation with an 808 nm laser (1 W/cm^2) for 5 minutes. The photothermal conversion efficiency (PCE) of Y6 NPs is determined using equation (3), as described previously.[3] The temperature change of Y6 NPs (1 mL) with an absorption intensity at 808 nm = 0.69 is obtained under 808 nm laser irradiation (1 W/cm^2). Once a plateau in temperature increase is reached, the laser is deactivated and the corresponding cooling temperature is recorded at intervals of every 30 seconds until the temperature returns to room temperature.

$$\eta = \frac{hS\Delta T_{max} - Q_{Dis}}{I(1 - 10^{-A_{808}})} \quad (4)$$

where h represents the heat transfer coefficient, S represents the container area, ΔT_{max} indicates the temperature difference between peak flat-state temperature and room temperature, Q_{Dis} indicates the heat relevant to the light absorbance of deionized water, I indicates the excitation power density, and A_{808} indicates the absorption intensity of Y6 NPs at 808 nm. hS can be obtained by equation (5).

$$\tau_s = \frac{m_D C_D}{hS} \quad (5)$$

where m_D represents the mass of water (1 g), and C_D represents the heat capacity of water (4.2 J/g). τ_s can be obtained by equation (5).

$$t = -\tau_s(ln\,\theta) \quad (6)$$

where θ is the ratio of ΔT to ΔT_{max}, ΔT is the temperature difference between the cooling temperature at 30 seconds intervals and room temperature. τ_s of Y6 NPs is determined to be 322 seconds. PCE of BTP-2TCF NPs is obtained in the same way, τ_s of BTP-2TCF NPs is determined to be 372 seconds.

8. Oscillator strength calculation using the Method of Moments

The oscillator strength is a dimensionless quantity that reflects the probability of

an electronic transition. It can be estimated using the following formula:

$$f = 4.317 \times 10^{-9} \int_{band} \varepsilon(\nu) d\nu \quad (7)$$

where f is the oscillator strength; $\varepsilon(\nu)$ is the molar extinction coefficient (in $M^{-1}cm^{-1}$) as a function of frequency ν (in cm^{-1}).

9. Detection of intracellular ROS generation

4T1 cells are seeded onto confocal dishes and incubated for a period of 24 hours. 4T1 is an aggressive murine breast cancer line that is widely used for *in vivo* studies, and it can form tumors in immunocompetent BALB/c mice as a standard syngeneic model. This makes it particularly suitable for establishing subcutaneous tumors for our NIR-II fluorescence imaging and photothermal therapy experiments. The culture medium is then replaced with BTP-2TCF NPs (26.7 μg/mL) and then incubated for another 4 hours. Subsequently, the medium is discarded and replaced by DCFH-DA (10 μM) and Hoechst 33342 (5 μM), followed by an additional incubation of 20 minutes. The laser-treated groups' cells are excited using an 808 nm laser (1 W/cm^2) for 5 minutes, after which the cells are washed three times by using PBS. Results are visualized using a laser confocal scanning microscope.

10. *In vitro* cytotoxicity studies

For cell counting kit 8 (CCK8) assay, A549/4T1 cells are seeded in 96-well plates at a density of 5000 cells each well. A549 is a well-characterized human lung adenocarcinoma line commonly used for *in vitro* evaluation, providing a representative human-derived model. Using two biologically and species-diverse cell lines allows us to assess the robustness and general applicability of our nanoparticles across different tumor types. After incubating for 24 hours, the culture medium is replaced with Y6 NPs/ BTP-2TCF NPs dispersed in DMEM at various concentrations (100 μL; 0, 1.7, 3.3, 6.7, 13.3, 26.7 μg/mL). Following a subsequent incubation period of 4 hours with the NPs, the laser-treated group is exposed to irradiation from an 808 nm laser for 5 minutes. After another 24 hours, the NP-containing medium is substituted with a water-soluble tetrazolium 8 (WST-8) solution consisting of WST-8 (10 μL) diluted in PBS-free DMEM (90 μL). The resulting mixture is then incubated for 1 hour before measuring its OD at 450 nm using a microplate reader. Additionally, live/dead cell staining experiments are also conducted to validate the CCK8 results.

11. *In vivo* NIR-II FLI-guided cancer phototherapy and biosafety evaluation

All animal experiments are performed in accordance with the guidelines approved by the ethics committee of Beijing Institute of Technology with license number BIT-EC-SCXK 2019-0010-228. Animal model establishment: The Balb/c mice utilized in the experiment are procured from GemPharmatech (Nanjing, China). All mice used are female, aged 6-8 weeks and weighing between 16-20 g. Subcutaneous injection of 80 μL cell suspension (24×10^7 cells/mL) is administered into the right leg of each mouse

to establish a 4T1 tumor-bearing model. Subsequent experimental procedures are conducted once the tumor volume reaches approximately 60-100 mm^3.

In vivo and *ex vivo* FLI: Mice with a tumor volume of ~100 mm^3 are randomly selected for *in vivo* FLI. Following isoflurane gas anesthesia, the NIR-II small animal FLI system is used to detect the fluorescence signal of the tumor, representing the 0-48 hour FLI result. Subsequently, BTP-2TCF NPs (100 μL, 0.5 mg/mL) are intravenously injected into the mice and the fluorescence signals in mice are recorded at 3, 6, 12, 24, 36, 48, and 72 hours respectively. The experimental results are analyzed using image J software. After determining that the highest time point for NP aggregation at the tumor site is at 36 hours post-injection, another 4T1 tumor-bearing mouse with a tumor volume of approximately 100 mm^3 received an injection of BTP-2TCF NPs (100 μL, 0.5 mg/mL) via tail vein administration. The mouse is euthanized after a period of 36 hours elapsed since injection. Subsequently, the main organs including the heart, liver, spleen, lung, and kidney as well as the tumor are dissected. The relative fluorescence intensity of different organs at this time point is detected and analyzed.

Phototherapy and biosafety: A total of 20 tumor-xenograft mice are randomly assigned to the following groups: PBS, PBS + Laser, BTP-2TCF NPs, and BTP-2TCF NPs + Laser. Subsequently, each mouse in these groups received a tail vein injection of 100 μL of either PBS (1×), or BTP-2TCF NPs (1.0 mg/mL). After 24 hours, the tumor sites of mice in the PBS + Laser group and BTP-2TCF NPs + Laser group are exposed to 5-minute irradiation from an 808 nm laser (0.5 W/cm^2). Infrared thermography using FLUKE TiR29 is employed to record temperature changes at the tumor site for mice in these two groups, enabling the construction of temperature change curves. On day zero corresponding to the day when treatment is administered, body weight changes and tumor volume alterations are monitored every two days across all experimental groups using the formula: volume = (length * $width^2$)/2.

After 14 days of treatment, the mice are euthanized in a CO_2 atmosphere. Blood samples are collected and analyzed using an animal-specific blood gas and electrolyte analyzer to assess routine blood indicators. The serum is obtained and tested using an animal-specific fully automated biochemical analyzer to evaluate blood biochemical parameters. Following dissection, tumor tissue weight is measured *ex vivo* on day 14. Organs including the heart, liver, spleen, lung, kidney, and tumor are extracted and fixed in a 4% paraformaldehyde solution for 24 hours. All organs undergo hematoxylin-eosin (H&E) staining analysis for biosafety assessment purposes. Besides, H&E staining along with terminal deoxynucleotidyl transfer-mediated dUTP Nick-end labeling assay staining is performed on tumors to evaluate treatment efficacy.

12. Statistical analysis

The optical spectra of Y6/ BTP-2TCF molecules, NPs, and crystals are normalized by Origin. Data shown are mean ± standard deviation. The sample size for each statistical analysis is listed in corresponding figure legends. One-way ANOVA with Tukey test is carried out across groups using Origin. In all cases, significances are defined as $p \leq 0.05$.

13. Synthesis of BTP-2TCF

12,13-bis(2-ethylhexyl)-3,9-diundecyl-12,13-dihydro-[1,2,5]thiadiazolo[3,4-e]thieno[2",3":4',5']thieno[2',3':4,5]pyrrolo[3,2-g]thieno[2',3':4,5]thieno[3,2-b]indole-2,10-dicarbaldehyde (BTP-Di-CHO) (100 mg, 0.09 mmol), 2-(3-cyano-4,5,5-trimethylfuran-2(5H)-ylidene)malononitrile (42 mg, 0.21 mmol), acetic acid (5 mL) and pyridine (1 mL) are added into a two-neck flask, then the reaction mixture is refluxed for 6 to 8 hours. The reaction mixture is monitored with TLC, and if the starting material not fully consumed then add 2-(3-cyano-4,5,5-trimethylfuran-2(5H)-ylidene)malononitrile (20 mg) and 0.5 mL of pyridine and reflux further 3 to 4 h. The reaction mixture is workup with dichloromethane and water, dried over $MgSO_4$, concentrated and purified by column chromatography on silica gel using DCM/MeOH (99:1, v/v) to obtain BTP-2TCF (83 mg, 62%) as a dark blue solid. ^{1}H NMR (400 MHz, $CDCl_3$) δ (ppm) 8.15 (d, *J* = 16.0 Hz, 2 H), 6.63 (d, *J* = 16.0 Hz, 2 H), 4.62 (d, *J* = 4 Hz, 4.0 H), 3.01 (bs, 4H), 2.06-1.98 (m, 2H), 1.90-1.77 (m, 16 H), 1.48-1.33 (m, 9H), 1.30-1.21 (m, 24 H), 1.13-1.06 (m, 5 H), 1.03-0.93 (m, 10 H), 0.89-0.83 (m, 6 H), 0.73-0.59 (m, 12 H). ^{13}C NMR (100 MHz, $CDCl_3$) δ (ppm) 175.70, 172.76, 147.37, 146.03, 144.93, 137.73, 137.43, 134.92, 132.86, 128.16, 127.61, 113.08, 112.17, 111.43, 111.35, 110.64, 96.83, 95.79, 56.09, 55.29, 40.10, 31.84, 30.18, 29.71, 29.56, 29.54, 29.46, 29.36, 29.27, 28.79, 27.59, 26.61, 23.10, 22.62, 14.07. HRMS (m/z, MALDI) calcd. for $C_{80}H_{96}N_{10}S_5$ 1388.6321, found: 1388.6803.

14. Supplementary figures and tables

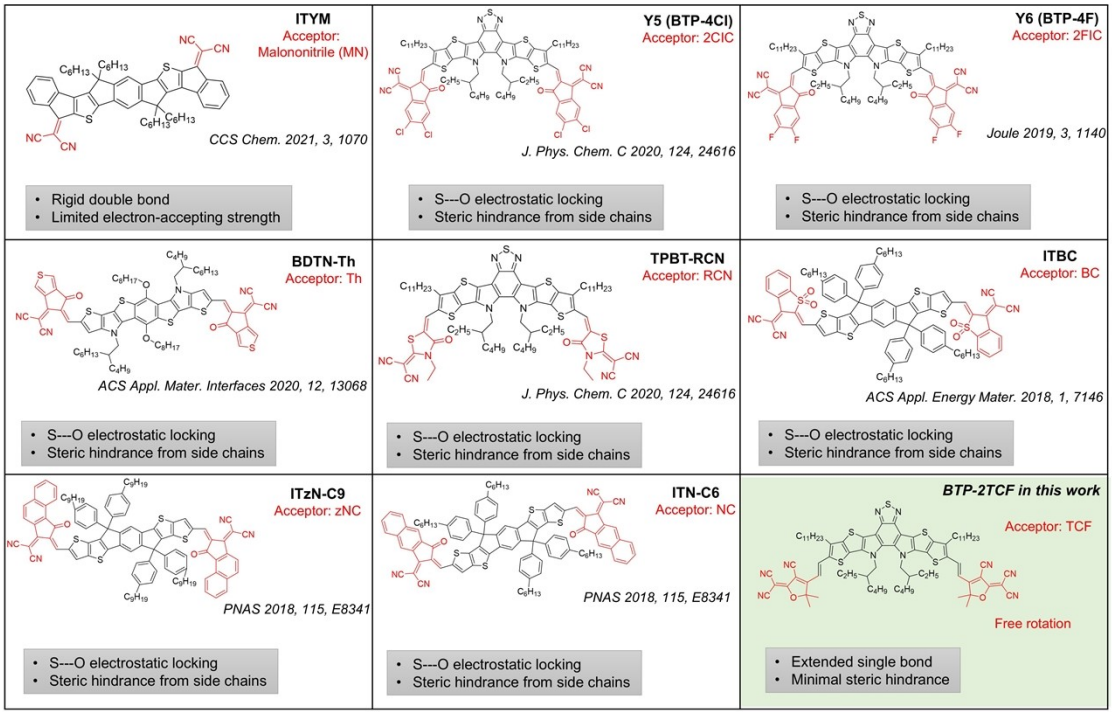

Figure S1. Summary of various non-fullerene acceptors in organic solar cells from recently published manuscripts.

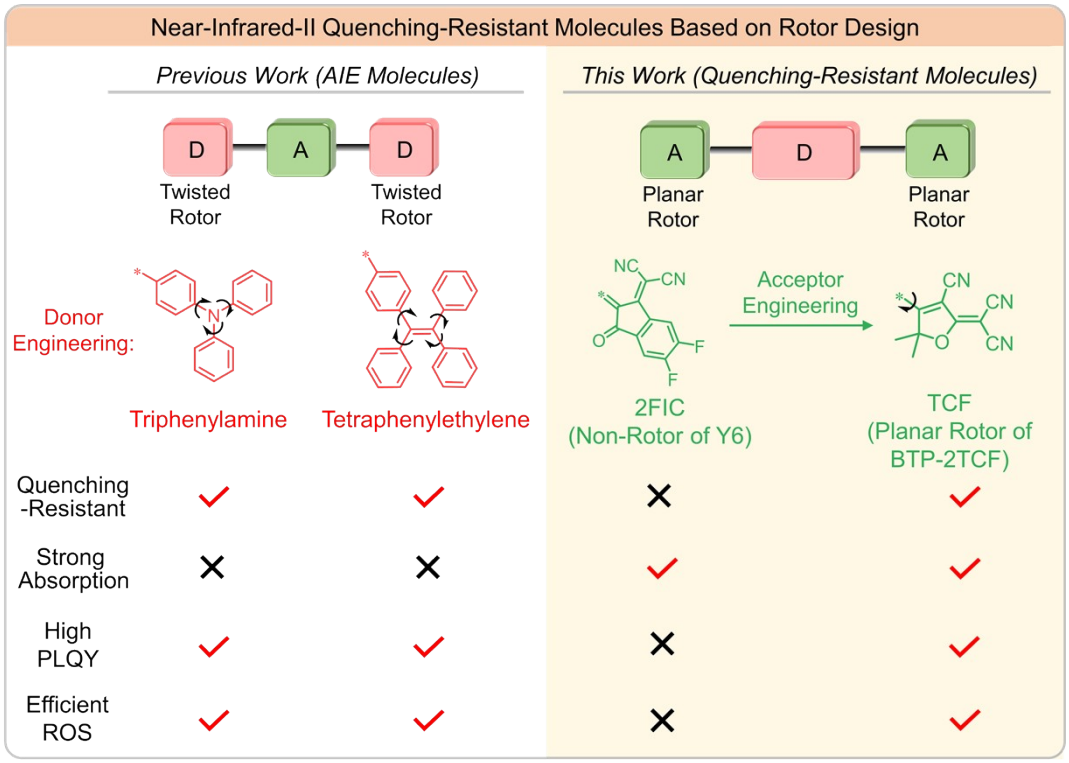

Figure S2. The scheme illustrating the properties of the previous reported AIE molecules, non-rotor molecules and developed quenching-resistant molecule in this work.

Table S1. Summary of photophysical parameters of recently reported state-of-the-art NIR-II AIE fluorophores and quenching-resistant molecule developed in this work.

	Samples	**ε_{808nm} ($M^{-1}cm^{-1}$)**	**Method to enhance ε**	**Φ_F (%)**	**Rotor Type**	**Brightness ($M^{-1}cm^{-1}$)**	**ROS generation**	**References**
AIE type	4TT-PBPT NPs	9,800	Dimerization	1.94	TPA	190	6.2 times of its counterpart	*Angew. Chem. Int. Ed.* ***2025,*** *137, e202417865*
	TEEITQ NPs	<16,800	Intramolecular electrostatic locking	0.26	TPE	<44	×	*Angew. Chem. Int. Ed.* ***2025,*** *64, e202413219*
	TSEH NPs	8,600	Intramolecular electrostatic locking	1.22	TPA	105	×	*Angew. Chem. Int. Ed.* ***2024,*** *63, e202404142*
	DTITBT NPs	<16,700	-	0.4	TPA	<67	5.7 times of its counterpart	*Adv. Mater.* ***2024,*** *36, 2306476*
	BT6 NPs	4,100	-	0.97	TPA	40	√	*Adv. Mater.* ***2023,*** *35, 2211632*
	TBTP-Au NPs	<25,800	Introducing heavy atom	0.092	TPA	<23	√	*Adv. Mater.* ***2023,*** *35, 2306616*

Anti-quenching type	BTP-2TCF NPs	33,400	Introducing planar rotor	1.7	TCF	635	10.2 times of Y6 NPs	*This work*

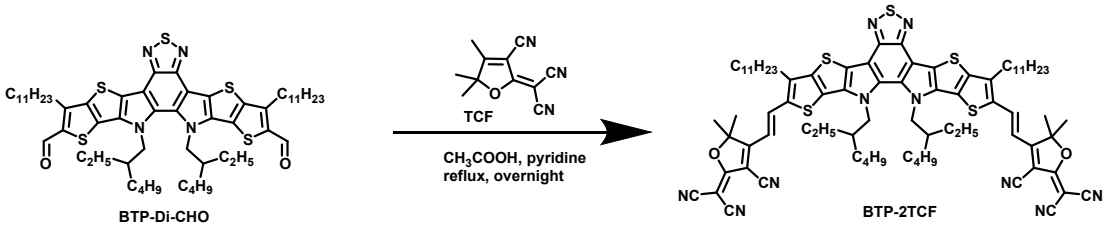

Scheme S1. Synthetic route toward fluorophore of BTP-2TCF.

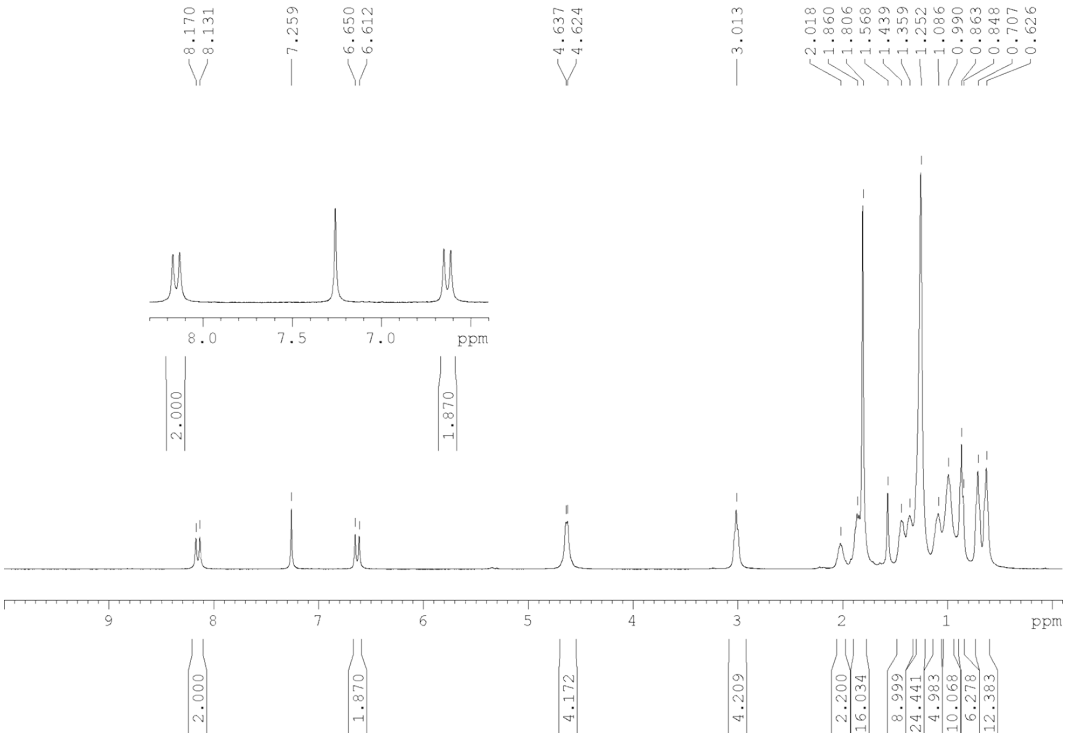

Figure S3. ^{1}H NMR spectrum of BTP-2TCF.

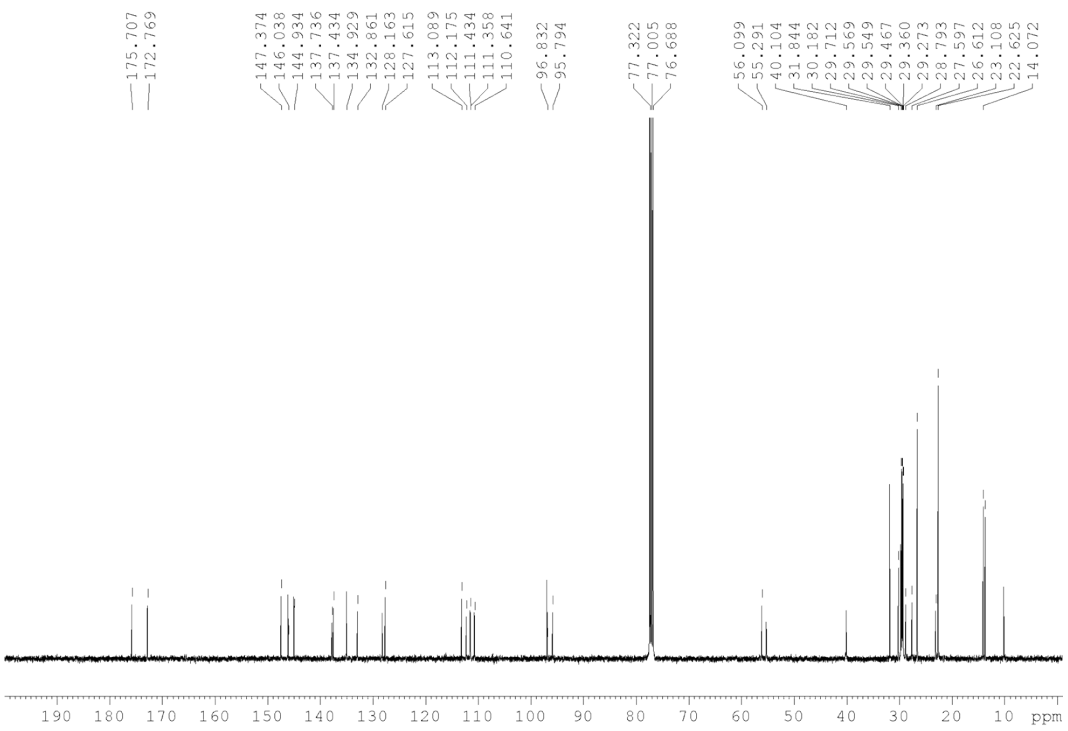

Figure S4. ^{13}C NMR spectrum of BTP-2TCF.

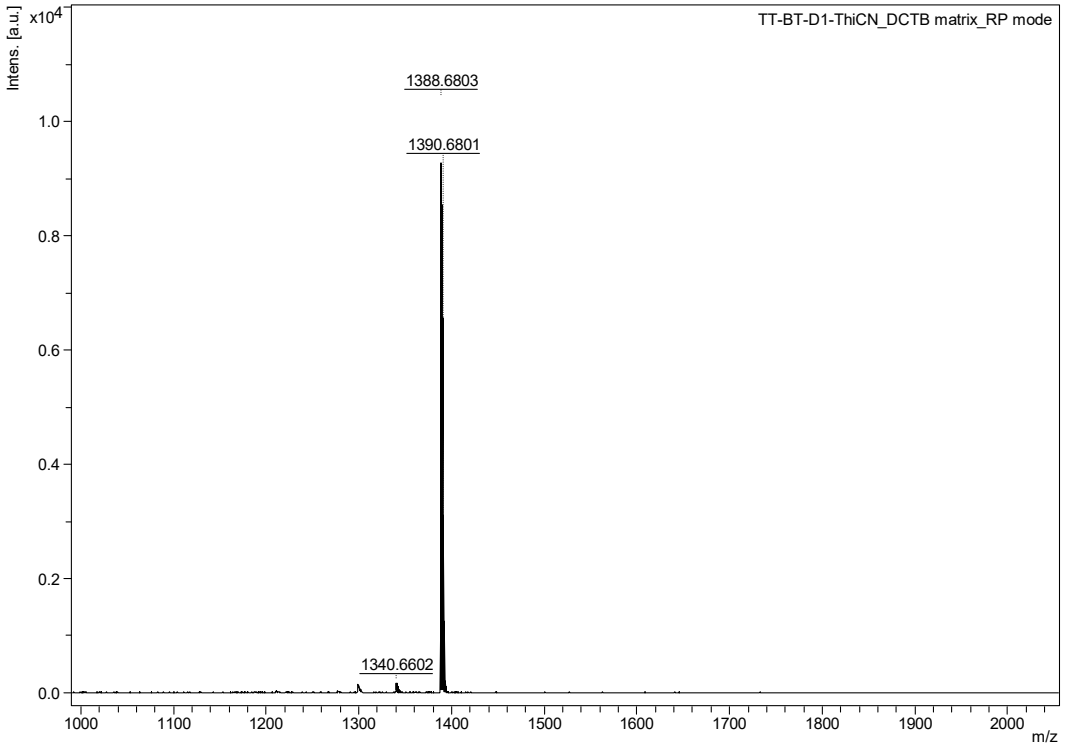

Figure S5. MALDI-TOF spectrum of BTP-2TCF.

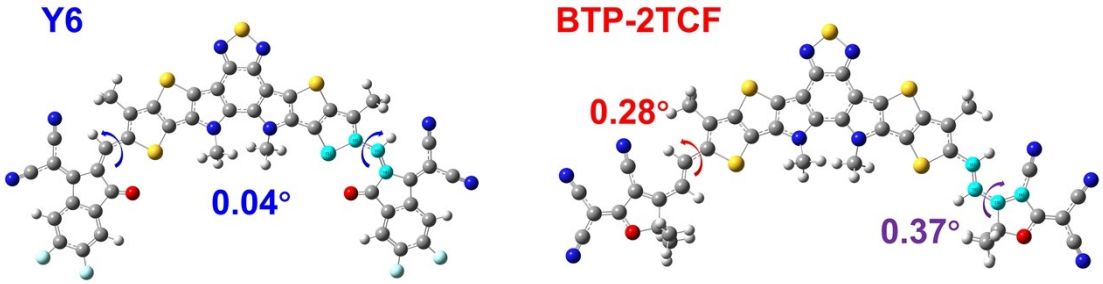

Figure S6. Dihedral angles of single bonds of Y6 and BTP-2TCF.

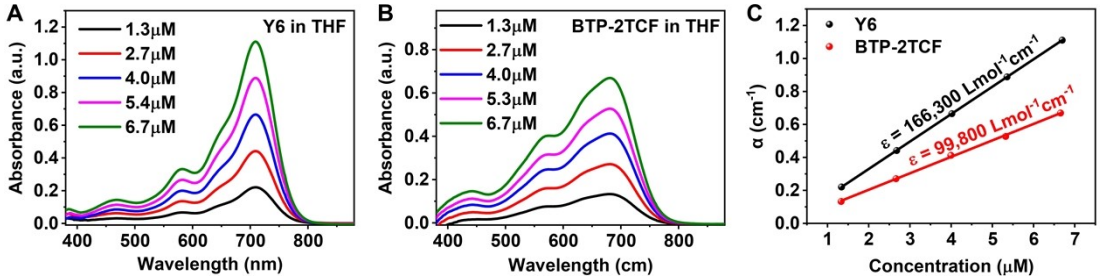

Figure S7. (A) Standard curve of Y6 and (B) BTP-2TCF in THF. (C) Plot of optical densities of absorption maxima against concentrations to determine molar extinction coefficient (Based on Least Squares Method; R^2: 1.000 for Y6, 0.999 for BTP-2TCF).

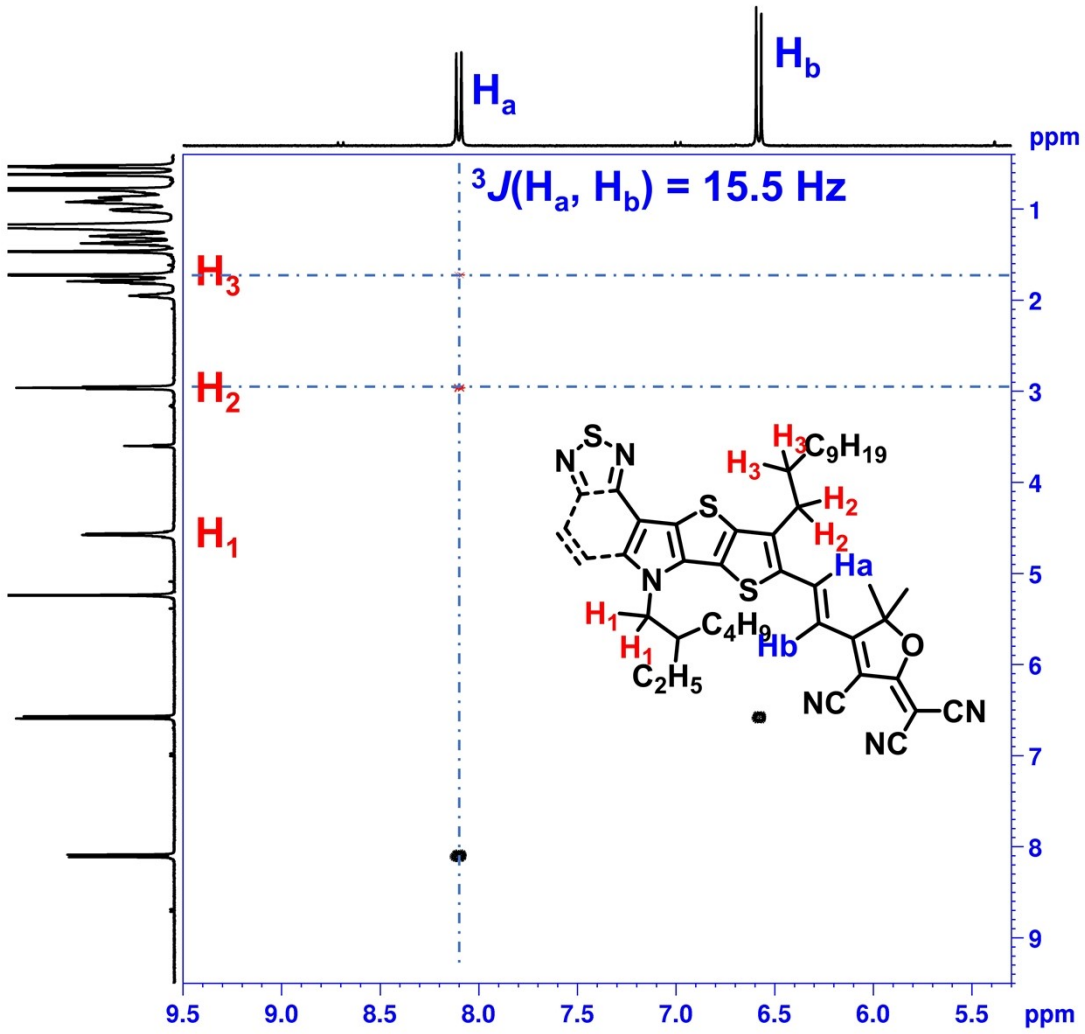

Figure S8. Assignment of the vinylic protons of BTP-2TCF in deuterated dichloromethane by 2D ^{1}H NMR spectrum.

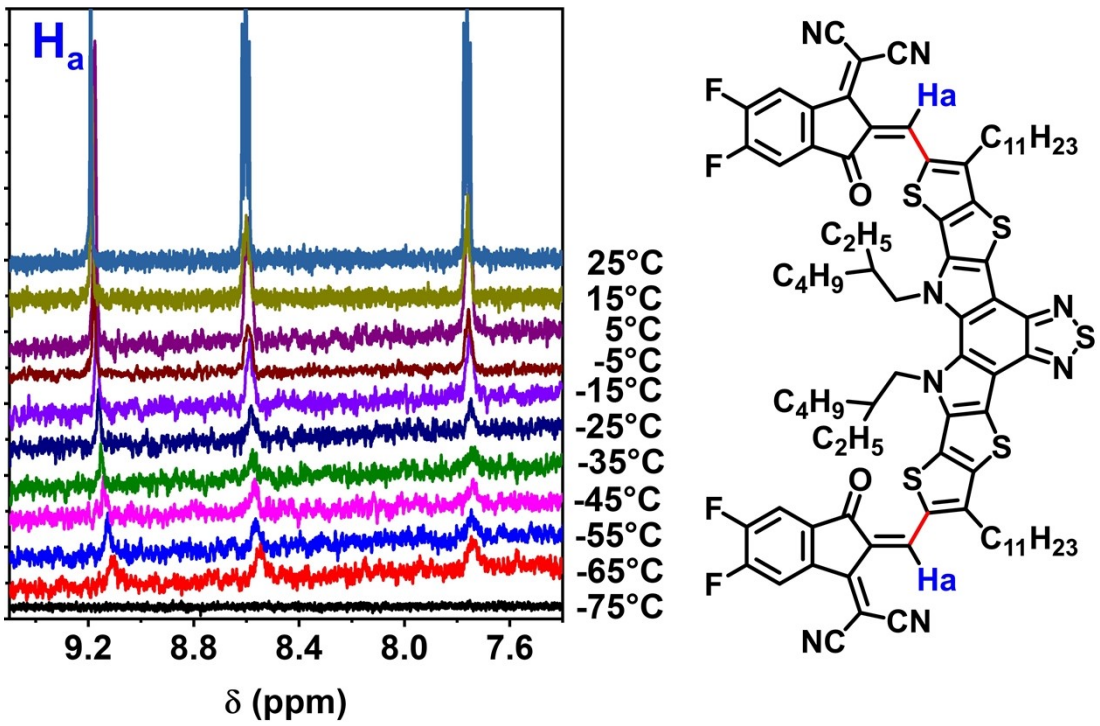

Figure S9. Evolution of the ^{1}H NMR spectrum aromatic part of Y6 with variable temperature (600 MHz, CD_2Cl_2).

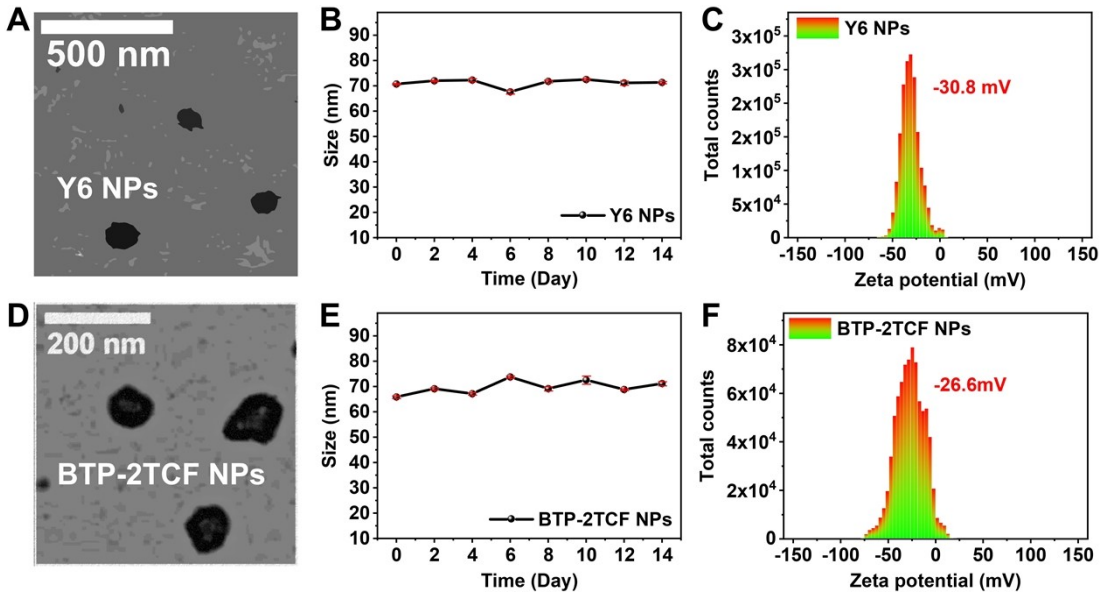

Figure S10. Preparation and characterization of NPs. (A) Morphology of prepared Y6 NPs obtained by TEM. (B) Size record of Y6 NPs dispersed in DI water for 14 days. (C) Zeta potential of prepared Y6 NPs dispersed in DI water. (D) Morphology of prepared BTP-2TCF NPs obtained by TEM. (E) Size record of BTP-2TCF NPs dispersed in DI water for 14 days. (F) Zeta potential of prepared BTP-2TCF NPs dispersed in DI water.

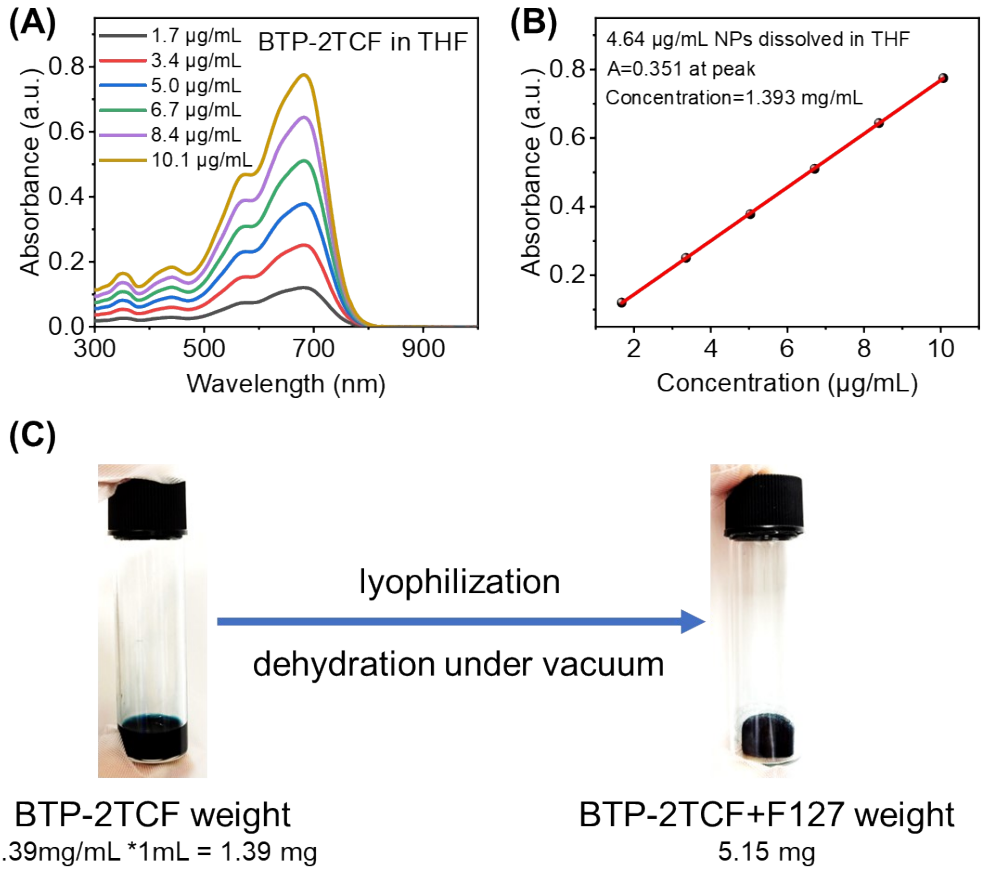

Figure S11. Measurement of drug-loading capacity of BTP-2TCF NPs. (A) Absorbance spectra of BTP-2TCF in THF at progressively increasing concentrations. (B) Determination of BTP-2TCF nanoparticle concentration by linear fitting of absorption maxima across varying concentrations. (C) Lyophilization procedure employed to quantify the combined mass of BTP-2TCF and F127 present in 1 mL of dispersion.

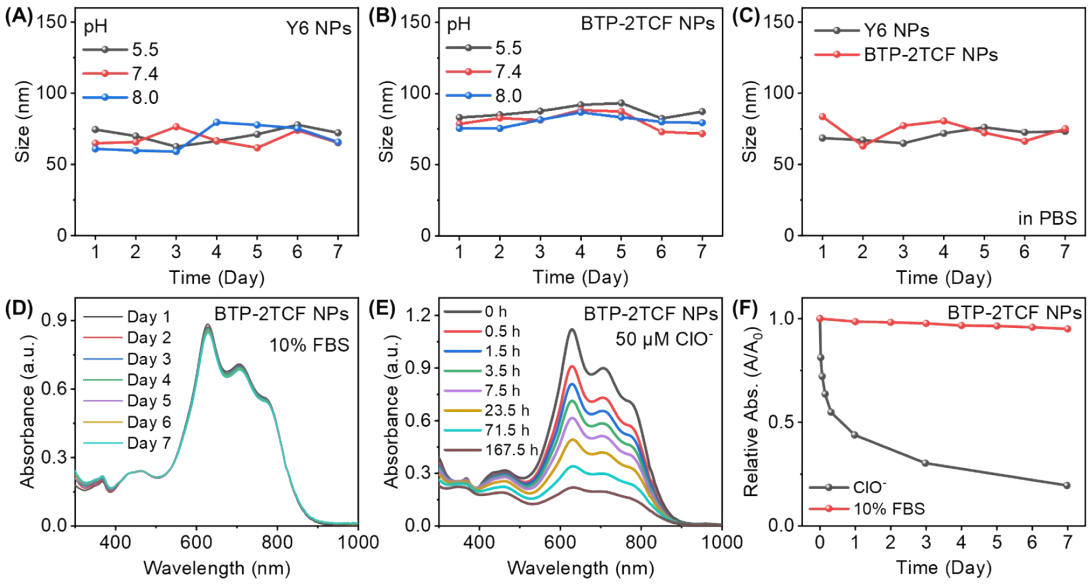

Figure S12. Dispersion stability tests under varying conditions. (A) Y6 NPs under different pH conditions (5.5, 7.4, 8.0); (B) BTP-2TCF NPs under different pH conditions (5.5, 7.4, 8.0); (C) Dispersion tests of Y6 NPs and BTP-2TCF NPs in PBS; Biodegradation behavior analysis. (D) Continuous monitoring of absorbance for BTP-2TCF NPs in 10% FBS solution; (E) Continuous monitoring of absorbance for BTP-2TCF NPs in PBS solution with 50 μM ClO^-; (F) Relative absorbance A/A_0 of BTP-2TCF NPs in 10% FBS and 50 μM ClO^- solutions.

Table S2. Summary of photophysical parameters of Y6 NPs and BTP-2TCF NPs in water.

	$\lambda_{max,\ abs}$ (nm)	$\lambda_{max,\ em}$ (nm)	PLQY (Φ_F, %)	ROS yield (%)	PCE (η, %)
Y6 NPs	802	936	1.2	4.3	54
BTP-2TCF NPs	628	936	1.9	7.9	49

Notes: Reference of PLQY measurement: IR-26 in DCE (0.5%); Reference of ROS yield measurement: ICG in water (0.2%)

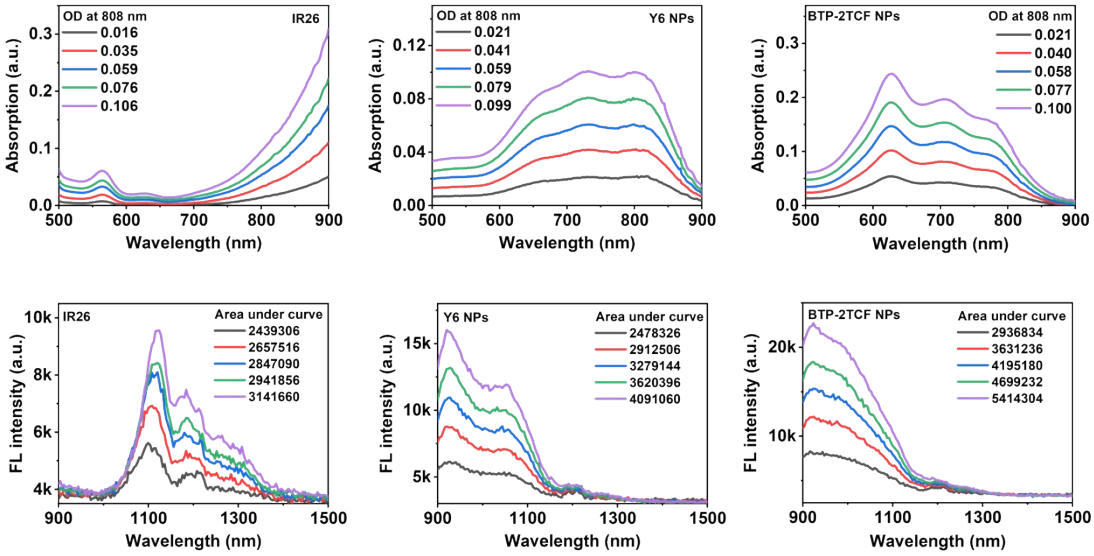

Figure S13. PLQY determination (n=1, PLQY of Y6 NPs: 1.1%(R^2=0.997), PLQY of BTP-2TCF NPs: 1.7%(R^2=0.996)) Absorption spectra of IR26 (A), Y6 NPs (B), and BTP-2TCF NPs (C) with OD values at 808 nm. Fluorescence spectra of IR26 (D), Y6 NPs (E), and BTP-2TCF NPs (F) with integrated NIR-II fluorescence intensities from 900-1500 nm. Excitation source: 808 nm laser.

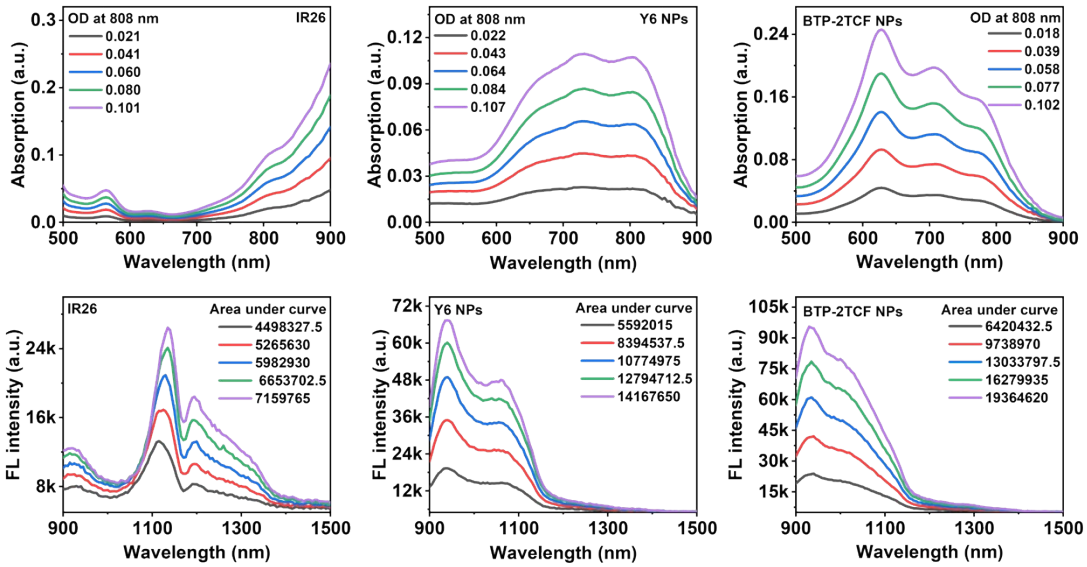

Figure S14. PLQY determination (n=2, PLQY of Y6 NPs: 1.3%(R^2=0.990), PLQY of BTP-2TCF NPs: 2.0%(R^2=0.996)) Absorption spectra of IR26 (A), Y6 NPs (B), and BTP-2TCF NPs (C) with OD values at 808 nm. Fluorescence spectra of IR26 (D), Y6 NPs (E), and BTP-2TCF NPs (F) with integrated NIR-II fluorescence intensities from 900-1500 nm. Excitation source: 808 nm laser.

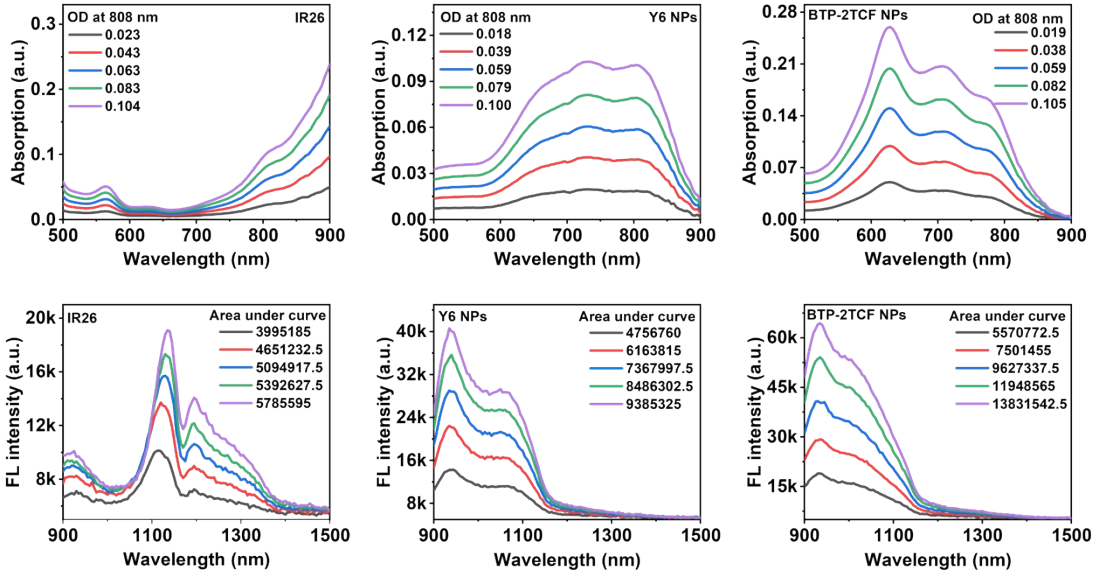

Figure S15. PLQY determination (n=3, PLQY of Y6 NPs: 1.1%(R^2=0.993), PLQY of BTP-2TCF NPs: 1.9%(R^2=0.998)) Absorption spectra of IR26 (A), Y6 NPs (B), and BTP-2TCF NPs (C) with OD values at 808 nm. Fluorescence spectra of IR26 (D), Y6 NPs (E), and BTP-2TCF NPs (F) with integrated NIR-II fluorescence intensities from 900-1500 nm. Excitation source: 808 nm laser.

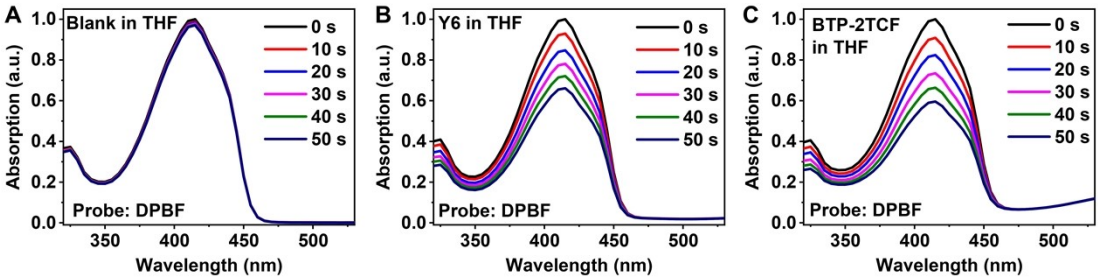

Figure S16. Singlet oxygen detection. Time-dependent absorption spectra of DPBF probe with DPBF only in THF (A), Y6 in THF (B), BTP-2TCF in THF (C) under 750 nm laser excitation (power density:160 mW/cm^2).

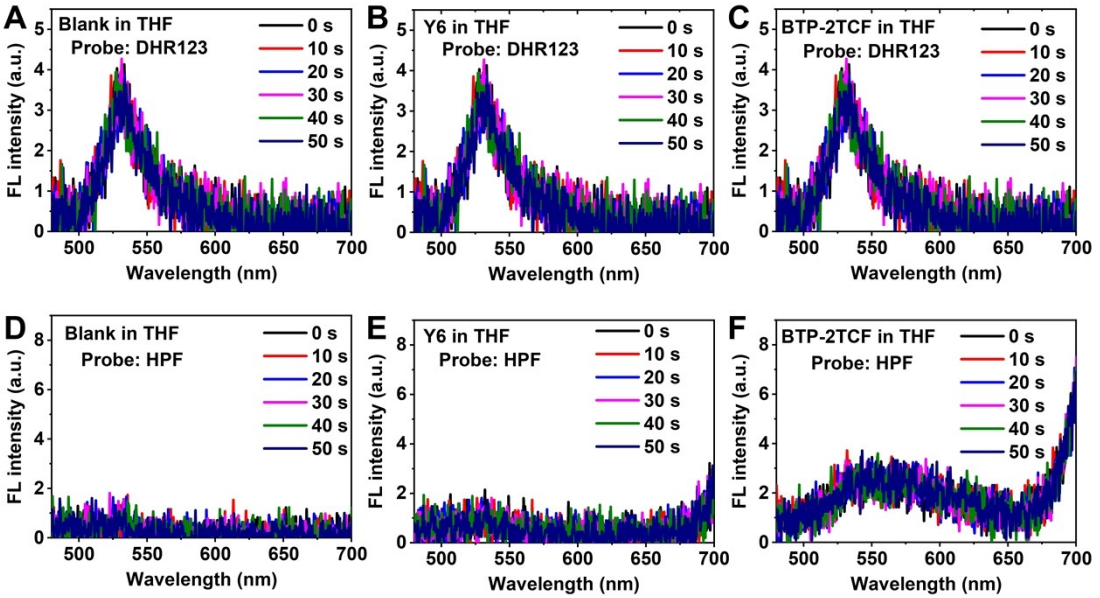

Figure S17. Superoxide radicals' detection(A-C). Time-dependent fluorescence spectra of DHR123 probe with DHR123 only in THF (A), Y6 in THF (B), and BTP-2TCF in THF (C) under 750 nm laser excitation (power density:160 mW/cm^2). Hydroxyl radicals' detection (D-F). Time-dependent fluorescence spectra of HPF probe with DHR123 only in THF (D), Y6 in THF (E), and BTP-2TCF in THF (F) under 750 nm laser excitation (power density:160 mW/cm^2).

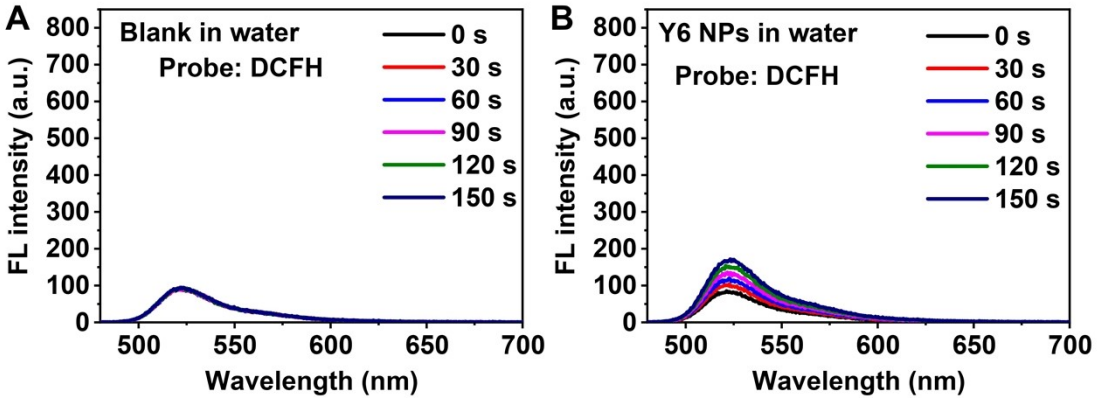

Figure S18. Time-dependent fluorescence intensity changes of DCFH with blank (A)

and Y6 NP (B) aqueous solution upon 808 nm irradiation (power density: 500 mW/cm^2).

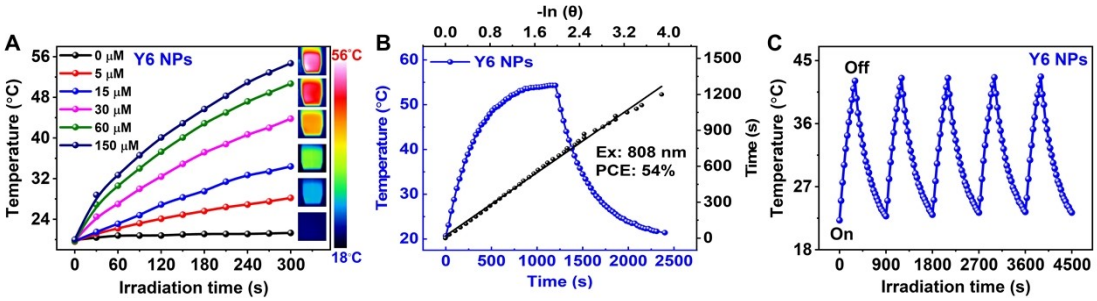

Figure S19. (A) Temperature-increasing curve of Y6 NPs with varied concentrations after 5 min of laser irradiation with corresponding infrared thermographs. (B) Temperature-increasing/decreasing curve and cooling time *vs* -ln(θ) plot of Y6 NPs. (C) Photostability tests of Y6 NPs for five cycles.

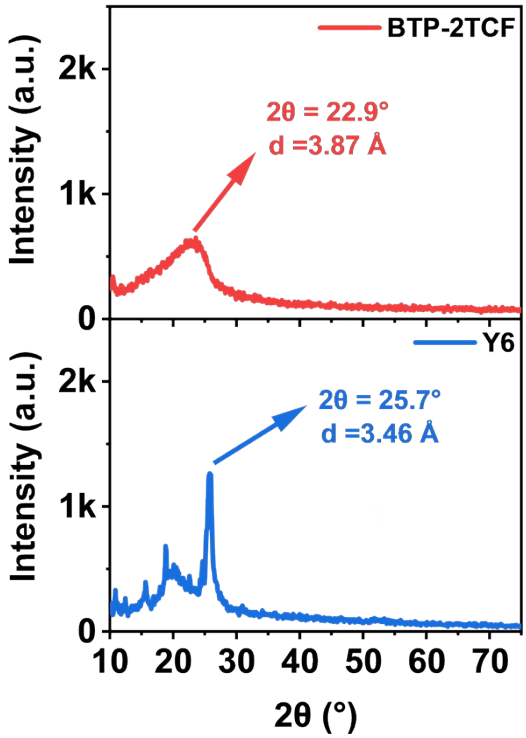

Figure S20. X-ray diffraction patterns of Y6 and BTP-2TCF powders under ambient conditions in air. The intermolecular spacing (*d*) values were calculated from the corresponding 2*θ* position using Bragg's law.

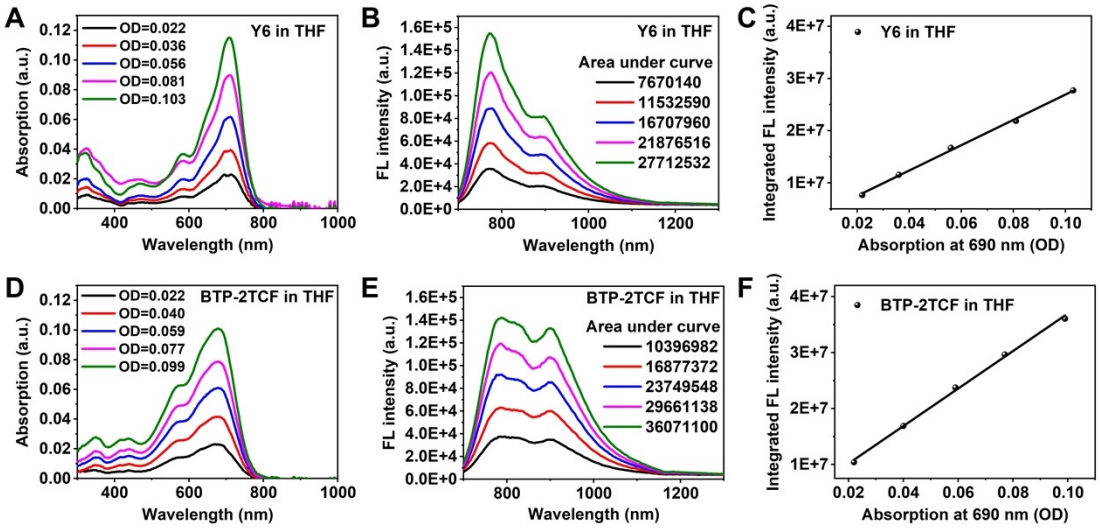

Figure S21. Absorption spectra of Y6 in THF (A) and BTP-2TCF in THF (D) with OD values at 690 nm. Fluorescence spectra of Y6 in THF (B) and BTP-2TCF in THF (E) with integrated NIR-II fluorescence intensities from 700-1300 nm. Excitation source: 690 nm xenon light. Plots of the integrated FL spectra of Y6 in THF (C) and BTP-2TCF in THF (F) at five different concentrations. (Based on Least Squares Method; R^2: 0.998 for Y6, 0.996 for BTP-2TCF)

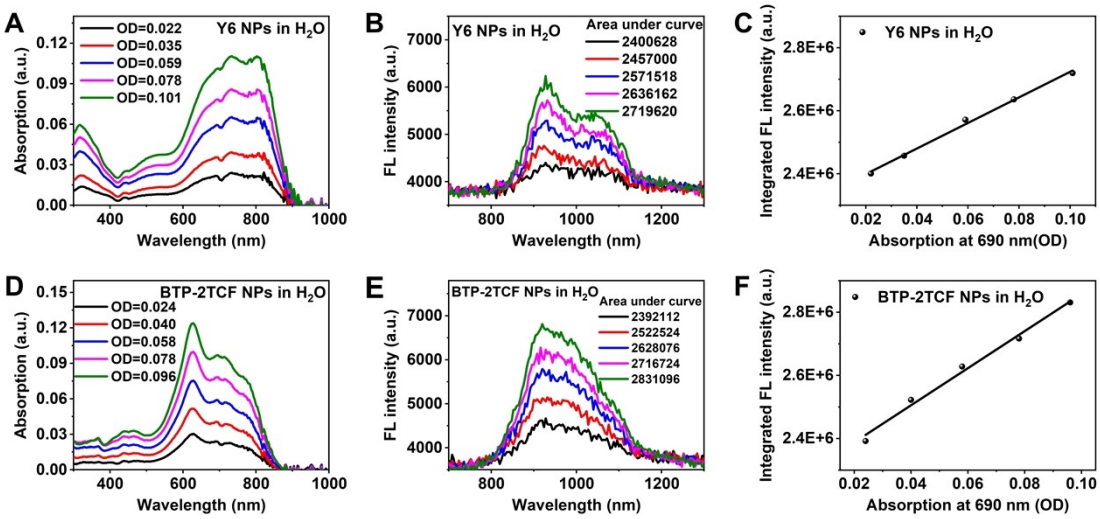

Figure S22. Absorption spectra of Y6 NPs in water (A) and BTP-2TCF NPs in water (D) with OD values at 690 nm. Fluorescence spectra of Y6 NPs in water (B) and BTP-2TCF NPs in water (E) with integrated NIR-II fluorescence intensities from 700-1300 nm. Excitation source: 690 nm xenon light. Plots of the integrated FL spectra of Y6 NPs in water (C) and BTP-2TCF NPs in water (F) at five different concentrations. (Based on Least Squares Method; R^2: 0.999 for Y6 NPs, 0.992 for BTP-2TCF NPs)

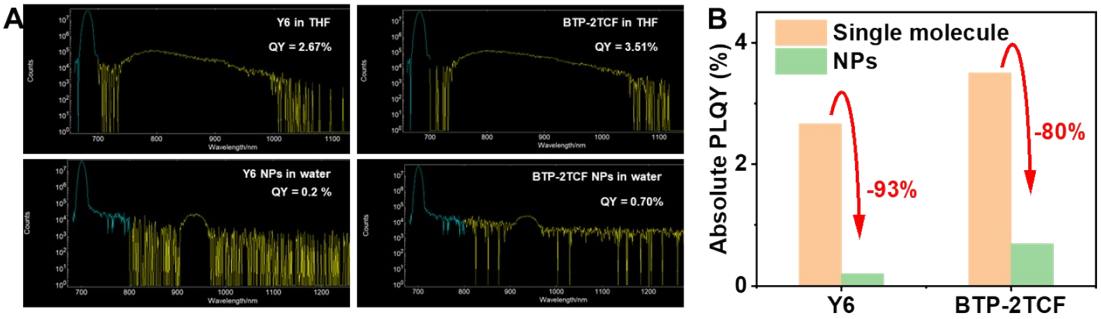

Figure S23. (A) Absolute PLQY measurements both for the solution and the NPs of Y6 and BTP-2TCF. (B) Comparison of anti-quenching behaviors between Y6 and BTP-2TCF from single molecule to their NPs.

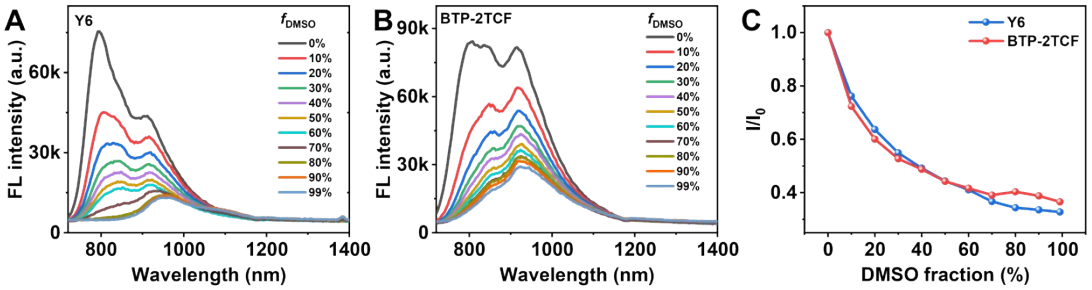

Figure S24. Photoluminescence spectra of Y6 (A) and BTP-2TCF (B) upon excitation at 690 nm, in a mixture of THF and DMSO with varying DMSO fractions (f_{DMSO}). (C) Normalized FL intensity variation with DMSO fraction in THF/DMSO mixtures.

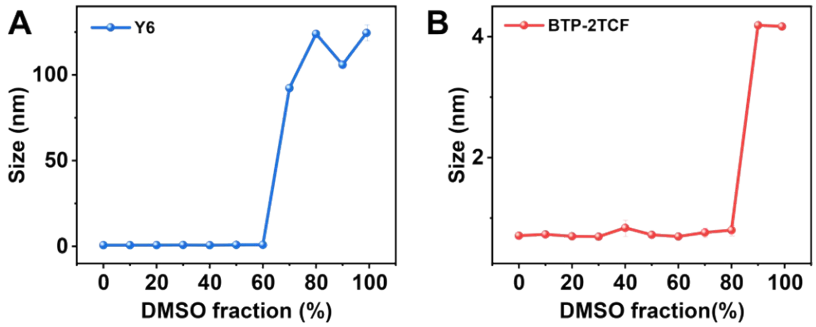

Figure S25. DLS measurement of Y6 (A) and BTP-2TCF (B) in a mixture of THF and DMSO with varying DMSO fractions (f_{DMSO}).

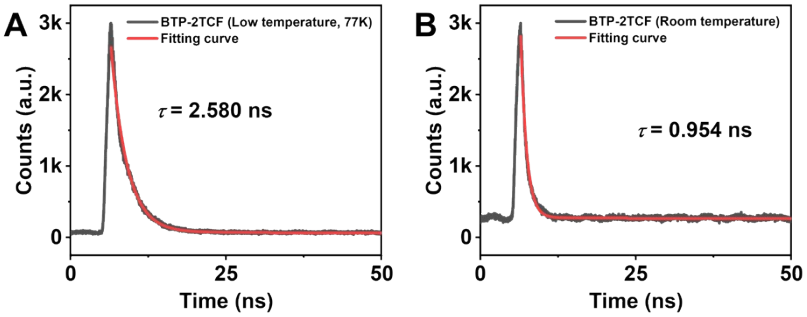

Figure S26. PL lifetimes of BTP-2TCF in toluene (670 nm EPL laser excitation;

lifetime detection wavelength: 780 nm). (A) Measurement under low temperature of 77K, fitting lifetime is 2.580 ns. (B) Measurement under room temperature of 298K, fitting lifetime is 0.954 ns.

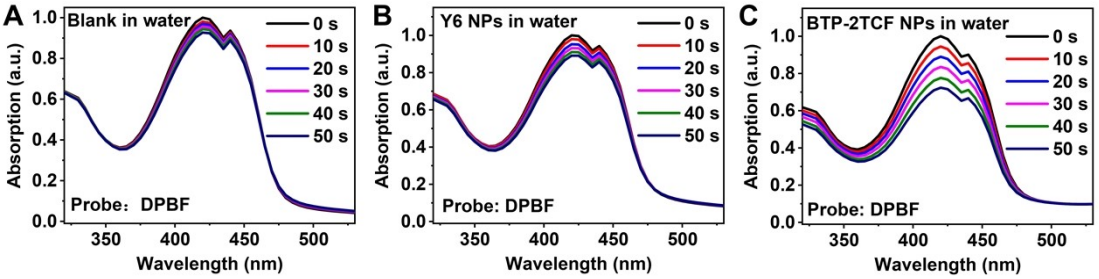

Figure S27. Singlet oxygen detection. Time-dependent absorption spectra of DPBF probe with DPBF only in water (A), Y6 NPs in water (B), BTP-2TCF NPs in water (C) under 750 nm laser excitation (power density:160 mW/cm^2).

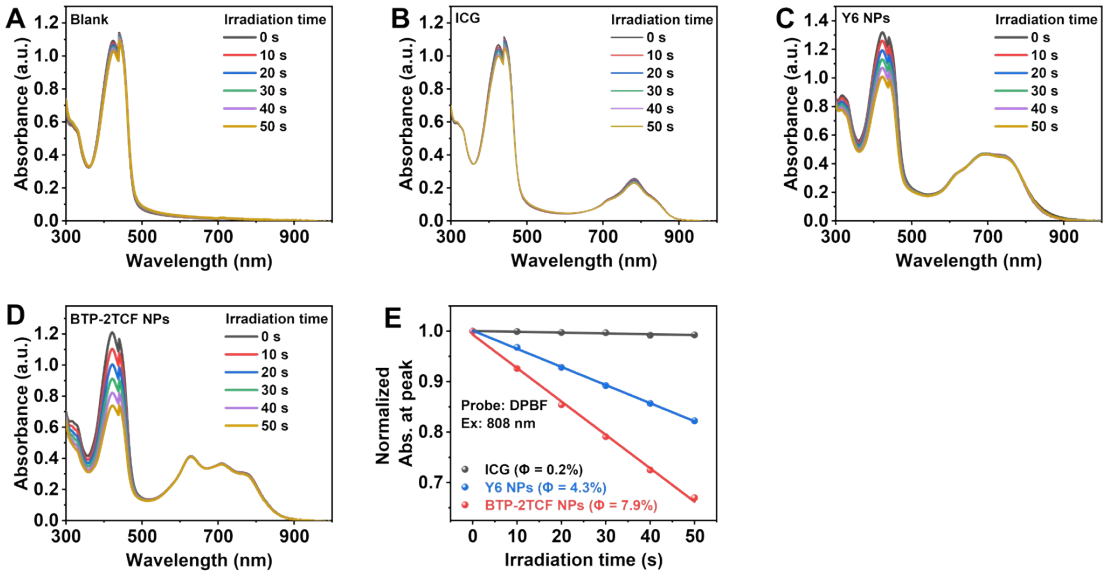

Figure S28. Quantitative singlet oxygen detection. Time-dependent absorption spectra of DPBF probe with DPBF only in water (A), ICG in water (B), Y6 NPs in water (C), BTP-2TCF NPs in water (D) under 808 nm laser excitation (power density: 200 mW/cm2). (E) Summary of data from A to D (Based on Least Squares Method; R^2: 0.901 for ICG, 1.000 for Y6 NPs, 0.998 for BTP-2TCF NPs).

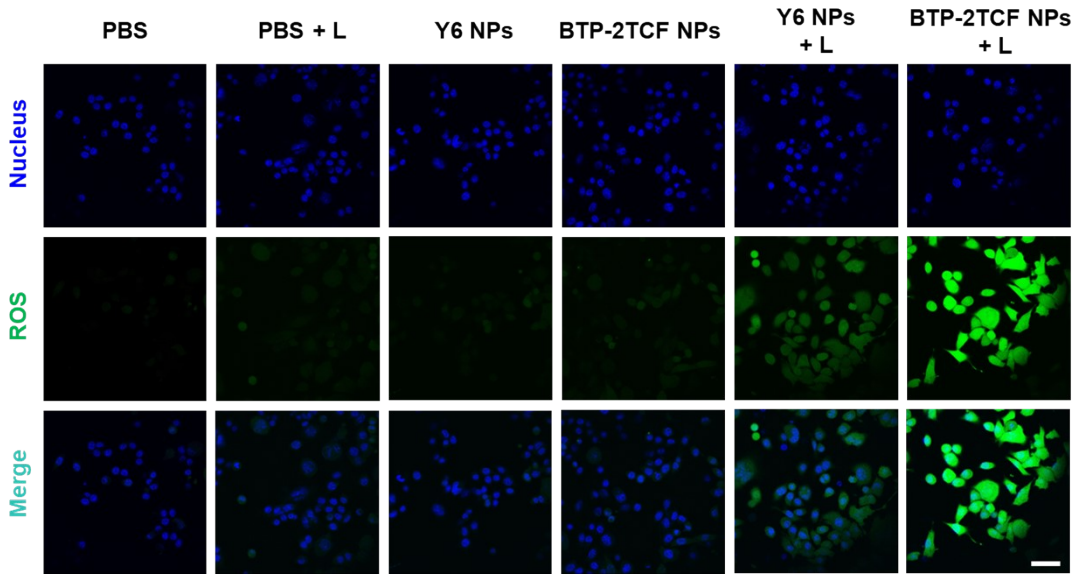

Figure S29. Confocal fluorescence images of ROS generation in 4T1 cells under various treatment conditions. (Probes: DCFH-DA for ROS detection and Hoechst 33342 for nuclear staining. NPs concentration: 26.7 μg/mL. Light irradiation: 808 nm laser, 0.33 W/cm^2, 15 min. Scale bar: 25 μm.)

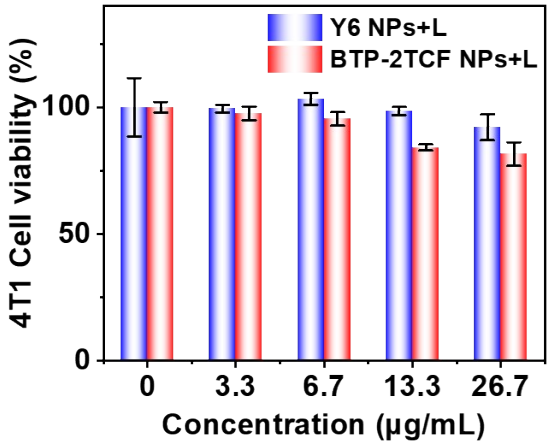

Figure S30. Cell viability of 4T1 cells treated with varying concentration of Y6 NPs and BTP-2TCF NPs with 808 nm laser irradiation (0.33 W/cm^2, 15 min). Data are presented as mean ± standard deviation (n = 4).

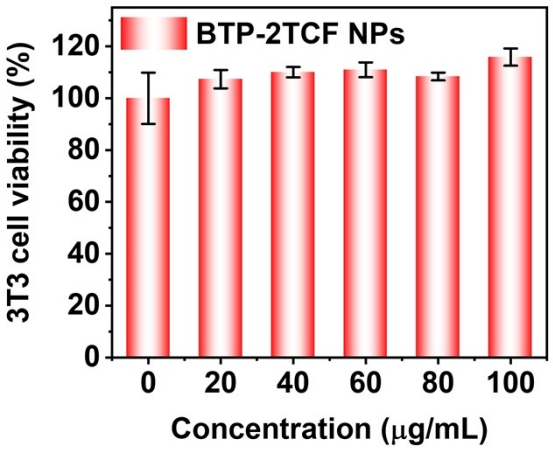

Figure S31. Dark toxicity of 3T3 cells incubated with BTP-2TCF NPs at different concentrations after 24 h.

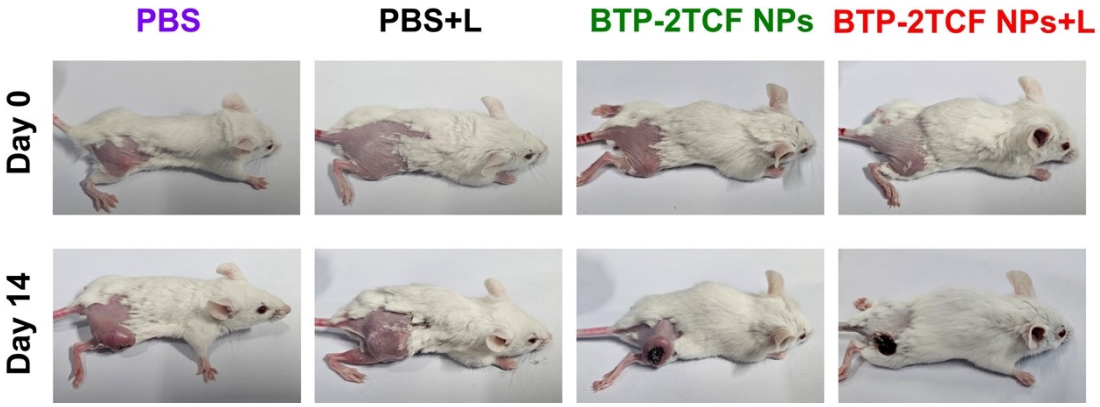

Figure S32. The images of mice being received different treatments on day 0 and day 14.

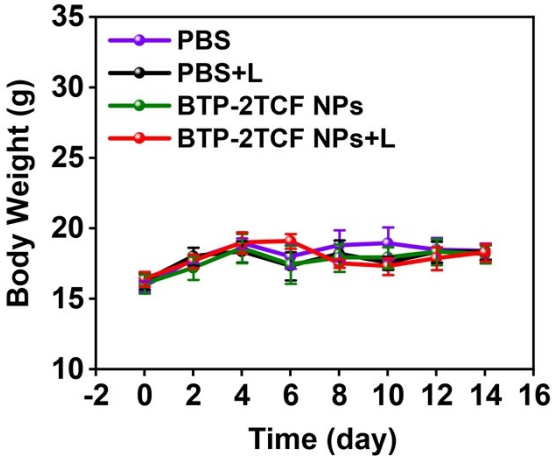

Figure S33. Body weight of the mice in different treatment groups (n = 5).

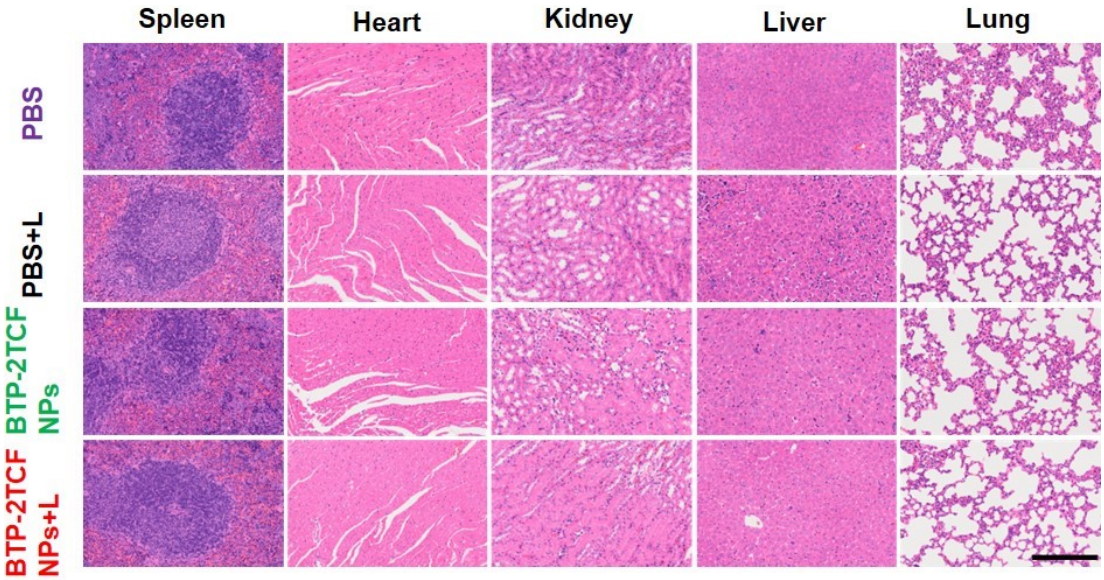

Figure S34. H&E staining of major organs excised from different treatment groups. Scale bar = 200 μm.

15. Reference

1. M. Frisch, G. Trucks, H. B. Schlegel, G. Scuseria, M. Robb, J. Cheeseman, G. Scalmani, V. Barone, G. Petersson and H. Nakatsuji, *Inc., Wallingford CT*, 2016, **2016**.
2. Y. Xu, C. Li, R. Xu, N. Zhang, Z. Wang, X. Jing, Z. Yang, D. Dang, P. Zhang and L. Meng, *Chem. Sci.*, 2020, **11**, 8157-8166.
3. K. W. Lee, Y. Gao, W. C. Wei, J. H. Tan, Y. Wan, Z. Feng, Y. Zhang, Y. Liu, X. Zheng and C. Cao, *Adv. Mater.*, 2023, **35**, 2211632.